

# The renal Na<sup>+</sup>/phosphate cotransporter NaPi-IIa is internalized via the receptor-mediated endocytic route in response to parathyroid hormone

D Bacic<sup>1,2</sup>, M LeHir<sup>2</sup>, J Biber<sup>1</sup>, B Kaissling<sup>2</sup>, H Murer<sup>1,3</sup> and CA Wagner<sup>1,3</sup>

<sup>1</sup>Institute of Physiology and Center for Integrative Human Physiology, University of Zurich, Zurich, Switzerland and <sup>2</sup>Institute of Anatomy, University of Zurich, Zurich, Switzerland

The major renal Na<sup>+</sup>/phosphate cotransporter, NaPi-IIa, is regulated by a number of factors including parathyroid hormone (PTH), dopamine, and dietary phosphate intake. PTH induces the acute internalization of NaPi-IIa from the brush border membrane (BBM) and its routing to and subsequent degradation in lysosomes. Previous work indicated that megalin, part of the apical receptor-mediated endocytic apparatus, may play a role in the PTH-induced removal of NaPi-IIa. Here we examined in rats the time-dependent internalization route of NaPi-IIa after acute PTH application using immunohistochemistry and markers of several endocytic compartments. NaPi-IIa removal from the BBM was detectable as early as 5 min after PTH injection. After 10–15 min, NaPi-IIa was localized in subapical compartments positive for clathrin. Shortly thereafter, NaPi-IIa appeared in endosomes stained for EEA1 (early endosomal antigen 1). After 45–60 min, NaPi-IIa was found in late endosomes/lysosomes marked with Igp120. In contrast, no change in the subcellular localization of megalin and the Na<sup>+</sup>/H<sup>+</sup> exchanger NHE3 was detected up to 60 min after PTH injection. To further characterize the internalization route, insulin, as a marker for receptor-mediated endocytosis, and horseradish peroxidase (HRP) and fluorescein isothiocyanate (FITC)-dextran (10 kDa), as markers for fluid-phase mediated endocytosis, were used. NaPi-IIa colocalized with insulin 5–30 min after PTH injection but did not overlap with HRP or FITC-dextran. These results demonstrate a distinct internalization route of NaPi-IIa in response to acute PTH application that may involve the receptor-mediated endocytic pathway including clathrin-coated vesicles and EEA1-positive early endosomes, and routes NaPi-IIa to lysosomes for degradation.

*Kidney International* (2006) **69**, 495–503. doi:10.1038/sj.ki.5000148; published online 6 January 2006

**Correspondence:** CA Wagner, Institute of Physiology, University of Zurich, Winterthurerstrasse 190, CH-8057 Zurich, Switzerland. E-mail: [wagnerca@access.unizh.ch](mailto:wagnerca@access.unizh.ch)

<sup>3</sup>These authors share last authorship.

Received 18 April 2005; revised 2 August 2005; accepted 15 September 2005; published online 6 January 2006

**KEYWORDS:** PTH; endocytosis; Na/phosphate-cotransporter; megalin; degradation

Inorganic phosphate (P<sub>i</sub>) homeostasis is effectively balanced between intestinal absorption via the Na<sup>+</sup>/phosphate cotransporter NaPi-IIb and the renal excretion regulated at the level of the apical Na<sup>+</sup>/phosphate cotransporters NaPi-IIa and NaPi-IIc.<sup>1</sup> Transport of P<sub>i</sub> across the proximal tubular apical membrane is mainly performed by NaPi-IIa.<sup>2,3</sup> A variety of stimuli regulate the abundance of NaPi-IIa and activity of Na/Pi cotransport including dietary phosphate intake, acid–base homeostasis, and a number of hormones such as parathyroid hormone (PTH), dopamine, and steroid hormones.<sup>1,3,4</sup> Rapid up- or downregulation of the transporter subsequent to acute changes in phosphate intake or PTH levels is based rather on post-transcriptional events, including intracellular trafficking, than on transcriptionally regulated changes in the mRNA levels of NaPi-IIa.<sup>1,3,5</sup> A decrease of proximal tubular reabsorption of phosphate (P<sub>i</sub>), which can be provoked by PTH, has been shown to correlate with a decrease in the number of type IIa Na/Pi cotransporters residing in the brush border membrane (BBM).<sup>2</sup> Internalization of NaPi-IIa *in vivo* most likely occurs at the invaginated membrane regions at the base of the BBM as demonstrated in PTH-treated rats.<sup>6</sup> Internalized NaPi-IIa proteins are subsequently directed to the lysosomes for degradation.<sup>6–8</sup> Similar observations were made in studies with OK cells, a cell line with some proximal tubular characteristics.<sup>7,9</sup>

In a first step of its rapid downregulation by PTH, NaPi-IIa accumulates transiently in the apical endocytic compartment of the proximal tubule before being degraded in a second step in the lysosomes within the course of one to several hours.<sup>7,8,10</sup> Similarities of this process with receptor-mediated endocytosis of ligands have been highlighted.<sup>10–13</sup> Previously, we have investigated NaPi-IIa internalization using immunohistochemical methods and found evidence for a distinct internalization route.<sup>6</sup> Moreover, we have recently demonstrated in two mouse models that loss of the endocytic receptor megalin itself or its chaperone protein RAP leads to an impairment and delay of the PTH-induced

NaPi-IIa internalization.<sup>14,15</sup> Taken together, these data point to a possible involvement of the receptor-mediated endocytic pathway in the internalization of NaPi-IIa in response to PTH.

However, little is known about the route of internalization and the underlying mechanisms of the rapid PTH-dependent removal of NaPi-IIa molecules and their subsequent intracellular routing to lysosomes. Therefore, the present study aimed to determine the route of retraction of NaPi-IIa *in vivo* after PTH treatment, employing confocal microscopy and dual labeling with markers of specific compartments such as clathrin-coated pits and endosomes together with markers for receptor-mediated and fluid-phase endocytosis. We used insulin as a representative marker for receptor-mediated endocytosis. Upon insulin binding, activated insulin receptors complexed with insulin are released from microvilli, segregate in clathrin-coated pits, and enter the cells. In endosomes, insulin is uncoupled from its receptor and the receptor recycles back to the cell surface, whereas insulin molecules are targeted to late endosomes and lysosomes where they are degraded.<sup>16</sup> Horseradish peroxidase (HRP) was used as a marker of fluid-phase endocytosis.<sup>13</sup>

The results indicate that the retracted NaPi-IIa molecules are following the pathway of receptor-mediated endocytosis being routed via clathrin-coated vesicles to early endosomes and lysosomes.

## RESULTS

A low- $P_i$  diet increases the expression of NaPi-IIa cotransporters predominantly in the brush border of superficial nephrons, the sites that under normal dietary conditions display a more moderate expression of the cotransporter.<sup>14,17</sup> Therefore, all animal experiments were performed on rats fed a low- $P_i$  diet for 3 days, in order to obtain maximal NaPi-IIa expression in all nephron generations as the starting point.

### Effect of PTH treatment on NaPi-IIa distribution

The method of injecting PTH into the vena cava in anesthetized rats allowed us to perform the hormone treatment for periods as short as 5 min and, without noticeable side effects from anesthesia, as long as 60 min. The initial immunohistochemical evaluation of the PTH effect at various time points (i.e. 5, 15, 30, and 60 min after injection) showed that the onset of NaPi-IIa internalization from the BBM was already detectable after 5 min and was very pronounced after 15 min. With prolonged treatment (30 and 60 min), the expression of NaPi-IIa cotransporters decreased in superficial as well as in juxtamedullary nephrons (Figure 1). NaPi-IIa in control animals showed almost exclusively BBM localization (the BBM was stained against actin in red, NaPi-IIa in green, overlay of NaPi-IIa and actin appeared in bright yellow). Higher magnifications of cross-sections of proximal tubules in PTH-injected rats illustrate that the intensity of the NaPi-IIa cotransporter staining (green label) was decreased in the BBM with prolonged PTH treatment (Figure 2). In PTH-injected animals, NaPi-IIa-

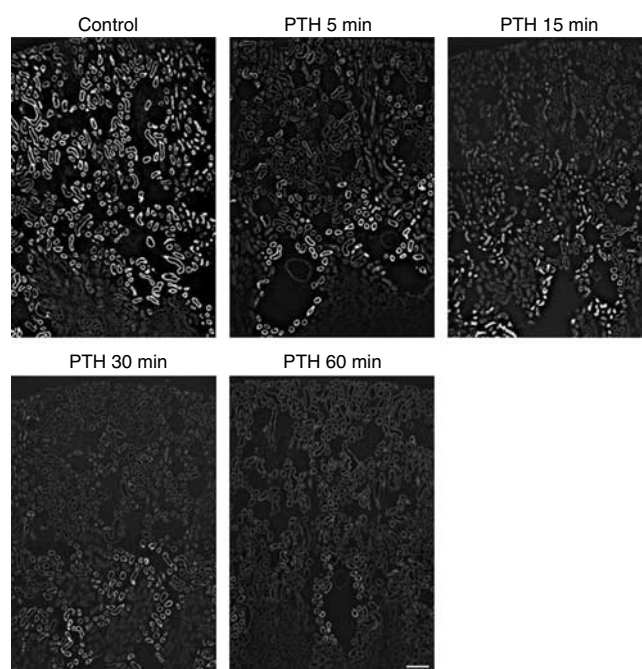


**Figure 1 | Type IIa NaPi cotransporter (NaPi-IIa) protein in the kidney cortex of control rats and of rats 5, 15, 30, or 60 min after injection with 1-34 PTH; cryostat sections, immunofluorescence.** NaPi-IIa labeling was strongly reduced in kidneys immediately 5 min after PTH application. After prolonged periods after PTH injection (15 and 30 min), NaPi-IIa staining remained strongest in proximal convoluted tubules of juxtamedullary nephrons, which almost completely disappeared 60 min after PTH administration. Bar = ~200  $\mu$ m.

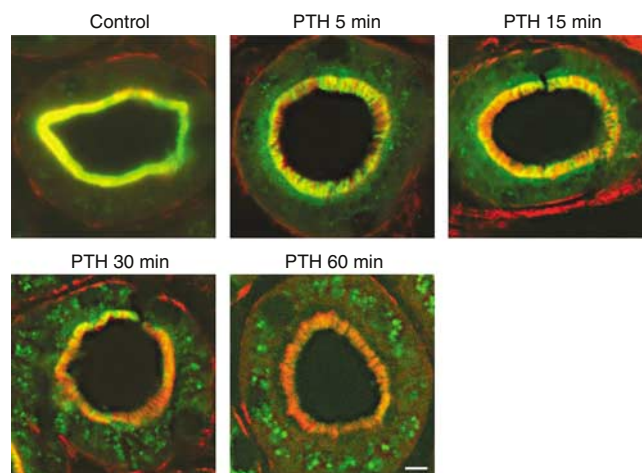


**Figure 2 | S1 segments of superficial nephrons stained with an antibody against NaPi-IIa (green label) and with rhodamine-phalloidin against  $\beta$ -actin filaments (red); cryostat sections, immunofluorescence.** Under control conditions, a high degree of overlap (yellow appearance) between NaPi-IIa and actin is seen, demonstrating the predominant localization of NaPi-IIa in the BBM. At 5–15 min after 1-34 PTH injection, the intensity of NaPi-IIa-related staining was decreased in the BBM (orange appearance) and a large green fluorescent rim appears below the BBM. Thirty minutes after PTH injection, the intensity of the intracellular NaPi-IIa staining (green) below the subapical region is increased. After 60 min, intracellular NaPi-IIa staining has disappeared and BBM was colored in red. Bar = ~10  $\mu$ m.

related immunostaining appeared in the subapical compartments and the intensity of the yellow staining faded and shifted toward red, indicating that the downregulatory effect of PTH on NaPi-IIa expression in the brush border. These observations are in agreement with previous data by us and others.<sup>10,14</sup>

#### Localization of NaPi-IIa in endocytotic compartments after PTH treatment

In order to identify the internalization route of NaPi-IIa to the lysosomes, we used antibodies against defined markers of several intracellular compartments known to be involved in the endocytic removal of membrane proteins (Figure 3). Shortly after PTH injection, NaPi-IIa staining (green label) moved to a subapical compartment, and started to colocalize with staining for clathrin (red label) below the brush border, indicating that the first steps in retrieval may involve clathrin-coated pits (Figure 3, after 5–15 min of PTH injection). Between 15 and 30 min after PTH treatment, colocalization of NaPi-IIa with clathrin became weaker, whereas vesicles labeled for NaPi-IIa showed frequently colocalization with the early endosomal antigen 1 (EEA1) (Figure 3, 15–30 min). To test whether internalized type IIa Na/Pi cotransporters under *in vivo* conditions are directed to the lysosomes, rats were treated with leupeptin to block lysosomal degradation before the treatment with PTH for 60 min. The distribution pattern of NaPi-IIa in the proximal tubule of control animals after leupeptin injection alone was in all respects identical to control animals that were not injected with leupeptin (data not shown). At 60 min after PTH injection, a strong overlap of internalized type IIa cotransporters with the late endosome/lysosome marker Igp120 was observed. In cortex sections obtained from rats infused with PTH but not pretreated with leupeptin, intracellular NaPi-IIa-related staining was found to be weaker (Figure 2, after 60 min of PTH injection), but still clearly present in late endosomes and lysosomes.

#### Distribution of NHE3 in kidneys of rats treated with PTH

To determine whether localization of the BBM-expressed Na<sup>+</sup>/H<sup>+</sup> exchanger NHE3 changes after acute treatment with PTH, dual labeling of NHE3 (green label) and  $\beta$ -actin (red label) was performed on cryosections from control and PTH-treated kidneys (Figure 4). Two different antibodies against NHE3<sup>18,19</sup> provided identical results. These results suggest that NHE3 is retracted to a domain at the base of the microvilli above the clathrin-coated vesicles in response to PTH treatment, but it does not move deeper in the cell. Our findings confirm a previous study by Yang *et al.*<sup>20</sup>

#### Effect of PTH on megalin localization in rat kidneys

We have previously shown that megalin, part of the receptor-mediated endocytic pathway (for review, see Christensen and Birn<sup>11,12</sup> and Willnow *et al.*<sup>21</sup>), may play an important role in the PTH-induced internalization of the NaPi-IIa.<sup>14,15</sup> Therefore, we examined the localization of megalin after PTH

treatment. It has already been shown that in the BBM, NaPi-IIa and megalin colocalize but during the PTH-induced internalization these two proteins do not share the same fate. After PTH injection, megalin (green label) was not detected by immunohistochemistry in clathrin- or EEA1-positive compartments (red label). Slight overlap (orange) of megalin and clathrin was found, due to localization of megalin in the deep invaginations of the BBM, where clathrin-coated pits are formed. There was no clear difference in the localization of megalin between untreated and PTH-treated animals (Figure 5).

#### Endocytosis of NaPi-IIa follows the receptor-mediated endocytic pathway

Two major routes of protein internalization from the apical membrane in the renal proximal tubule have been described: the receptor-mediated and the fluid-phase endocytic routes.<sup>11,12</sup> In order to identify the route of NaPi-IIa internalization, we used insulin and HRP as markers of the receptor-mediated and fluid-phase routes, respectively. In a first series of experiments, we found strong labeling of reabsorbed endogenous insulin in the proximal tubule. Therefore, rats were fasted for 18 h before the experiments in order to lower endogenous plasma levels of insulin to be able to detect the exogenously administered insulin (Figure 6). The localization of NaPi-IIa was not affected by the injection of insulin over a period of 5–30 min (data not shown). Animals were coinjected with PTH and insulin for different time points. Dual labeling of NaPi-IIa (green label) and insulin (red label) showed a strong overlap of these two proteins in endocytic compartments (granular orange-yellow staining), indicating that NaPi-IIa may have been endocytosed via receptor-mediated endocytosis (Figure 7 and Figure 10). Kidney sections from rats injected with the fluid-phase endocytic markers HRP or fluorescein isothiocyanate (FITC)-dextran (7 kDa) coinjected with PTH were double-labeled with NaPi-IIa (green label) and HRP or FITC-dextran (red label). HRP or FITC-dextran injection alone had no influence on the pattern of NaPi-IIa staining pattern (data not shown). The results demonstrated retrieval of NaPi-IIa from the BBM, but NaPi-IIa-related staining did only weakly overlap with HRP-labeled or FITC-dextran-containing endosomes (Figures 8–10). A direct comparison at higher magnification of NaPi-IIa with insulin- and HRP-labeled compartments showed a high degree of colocalization of NaPi-IIa with insulin but not HRP-containing vesicles (Figure 10).

#### DISCUSSION

In the present study, we traced the internalization pathway of the Na<sup>+</sup>/phosphate cotransporter NaPi-IIa in proximal tubular cells *in vivo* using immunofluorescence microscopy and employing specific markers of different endocytic pathways and compartments. The high degree of overlap of NaPi-IIa with endocytosed insulin indicates that NaPi-IIa is removed from the BBM by receptor-mediated endocytosis.



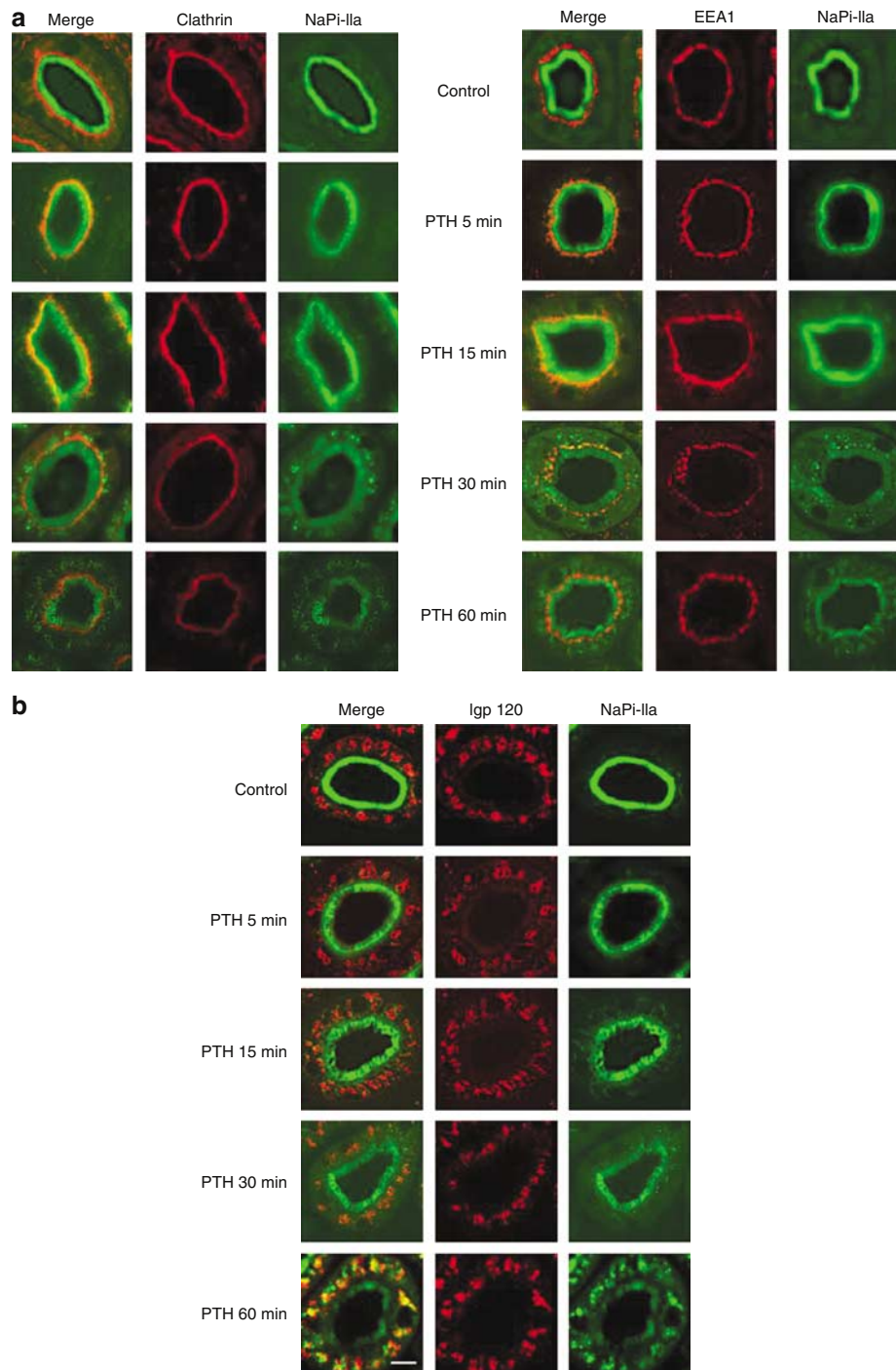


**Figure 3 | Colocalization of NaPi-IIa (green label) with clathrin, EEA1, and the lysosomal marker Igp120 (red label); cryostat sections, immunofluorescence. (a,b)** All pictures were taken from the S1 segments of superficial nephrons. At 5 and 15 min after PTH application, vesicles were colabeled for NaPi-IIa and clathrin (orange/yellow). Thirty minutes after treatment of animals with PTH, NaPi-IIa molecules were detected in deeper subapical regions and an overlap of internalized type II cotransporters with EEA1 was observed (orange/yellow). In sections of kidneys where 45 min after leupeptin injection PTH was administered for 60 min, NaPi-IIa-related immunofluorescence was absent from the BBM and subapical compartment. Intracellular NaPi-IIa-related staining increased and to a large extent overlapped with the distribution pattern of the late endosome/lysosome marker Igp120 (orange/yellow). Bar =  $\sim 15 \mu\text{m}$ .

This is corroborated by the previously demonstrated importance of the endocytic receptor megalin. Indeed, the acute internalization of NaPi-IIa in response to PTH was delayed in mice deficient for RAP, a chaperone of megalin, or

in mice with a kidney-specific reduction in megalin expression.<sup>14,15</sup> However, the experiments did not allow to distinguish between a direct participation of megalin in NaPi-IIa internalization and a more general disruption of the

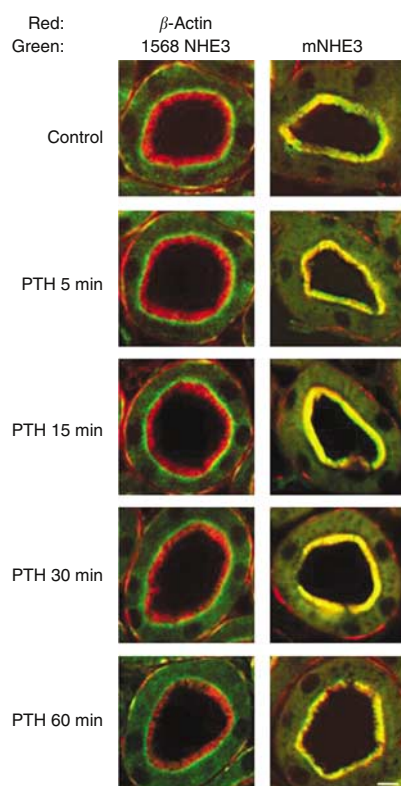


**Figure 4 | Effect of acute PTH application on NHE3 distribution; cryostat sections, immunofluorescence.** Rats were injected with PTH and kidneys fixed after 5, 15, 30, or 60 min. No difference in NHE3-related staining was detected between untreated control rats and rats injected with 1-34 PTH. Two different antibodies against NHE3 were used: a rabbit polyclonal antibody that recognizes NHE3 mainly at the bottom and deep invaginations of the BBM (upper panel) and a monoclonal anti-NHE3 antibody that stains NHE3 along the whole length of the BBM (lower panel). Under all conditions, distribution of NHE3 in the BBM appeared unchanged. NHE3 is stained in green and  $\beta$ -actin filaments in red. Bar =  $\sim 10 \mu\text{m}$ .

apical endocytic apparatus due to loss of megalin. Megalin serves as a receptor for the endocytosis of multiple ligands in the proximal tubule.<sup>11,12,14,15</sup> Reduction or loss of megalin expression and function is associated in mouse models and patients (Fanconi type syndromes) with urinary loss of vitamin D<sub>3</sub>, albumin, and other smaller proteins resulting in the disturbance of whole body calcium homeostasis and bone development.<sup>22–24</sup> In addition to its role in endocytosis of proteins from the urine, it has been suggested that megalin may directly interact with proteins in the BBM such as the Na<sup>+</sup>/H<sup>+</sup> exchanger NHE3 and may be important for the regulation and expression of this protein by mediating its endocytosis and membrane recycling.<sup>25</sup> In the BBM, NaPi-IIa and megalin colocalize,<sup>14,15</sup> but during the PTH-induced internalization these two proteins do not share the same fate. Megalin is recycled back to the membrane via dense apical tubules,<sup>12</sup> whereas NaPi-IIa is degraded in the lysosomes.<sup>6–9</sup> As, after injection of PTH, megalin could not be detected in clathrin- or EEA1-positive compartments, potential inter-

actions between megalin and NaPi-IIa may have occurred at an earlier time point during internalization. It is noteworthy that there is no evidence yet for a direct protein–protein interaction of NaPi-IIa and megalin (Gisler, Biber, Murer, unpublished results).

Whereas the results presented above indicate that the receptor-mediated endocytosis is involved in the rapid internalization of NaPi-IIa in response to PTH, no evidence was found for an involvement of the fluid-phase endocytic pathway. Indeed, HRP or FITC-dextran and NaPi-IIa did not show any significant overlay at any time point investigated. This is in contrast to a previous report suggesting that NaPi-IIa may be internalized via an HRP-accumulating compartment.<sup>6</sup> These findings had been based on indirect immunofluorescence and immuno-gold labeling. In view of the low grade of overlap between FITC-dextran or HRP with NaPi-IIa found here, these earlier findings may be explained either by a low amount of NaPi-IIa being internalized also via the fluid-phase-dependent endocytic pathway (which cannot be detected by indirect immunofluorescence) or by an unspecific binding of antibodies during immuno-gold detection.

The receptor-mediated endocytic pathway involves clathrin-coated vesicles, which fuse with the cisterns and tubes (‘early endosomes’) of the vacuolar apparatus, situated in the subapical compartment. From there, both insulin and NaPi-IIa were targeted via large endocytotic vacuoles (‘late endosomes’) into lysosomes. The involvement of clathrin is supported by previous studies on OK opossum kidney cells showing a reduced rate of endocytosis of NaPi-IIa by high medium osmolarity, the condition under which the endocytic mechanism is impaired.<sup>26</sup> Clathrin-mediated endocytosis plays an important role in regulating the membrane expression of other transport systems, for example, the vasopressin-dependent water channel aquaporin-2 in collecting duct principal cells and LLC-PK<sub>1</sub> cells.<sup>27,28</sup>

We were unable to observe an acute internalization of NHE-3 from the BBM in the rat model presented in this study. These results confirmed previous observations from our lab in mice and rats<sup>14,15</sup> (unpublished data) and from a recent publication by Yang *et al.*,<sup>20</sup> where clear evidence was provided for the PTH-induced retrieval of NHE3 from the top of the brush border microvilli to the intermicrovillar cleft region, but not its internalization. However, we cannot exclude that a small number of NHE3 exchangers was internalized but could not be detected by our methods.

In summary, we provide evidence that NaPi-IIa is internalized after acute application of PTH using a pathway overlapping with markers of the receptor-mediated endocytosis, but not fluid-phase endocytosis. This endocytic route includes clathrin-coated vesicles and early and late endosomes, and traffics NaPi-IIa to lysosomes for degradation. Previous evidence supports these data demonstrating the critical role of an intact apical apparatus for receptor-mediated endocytosis.

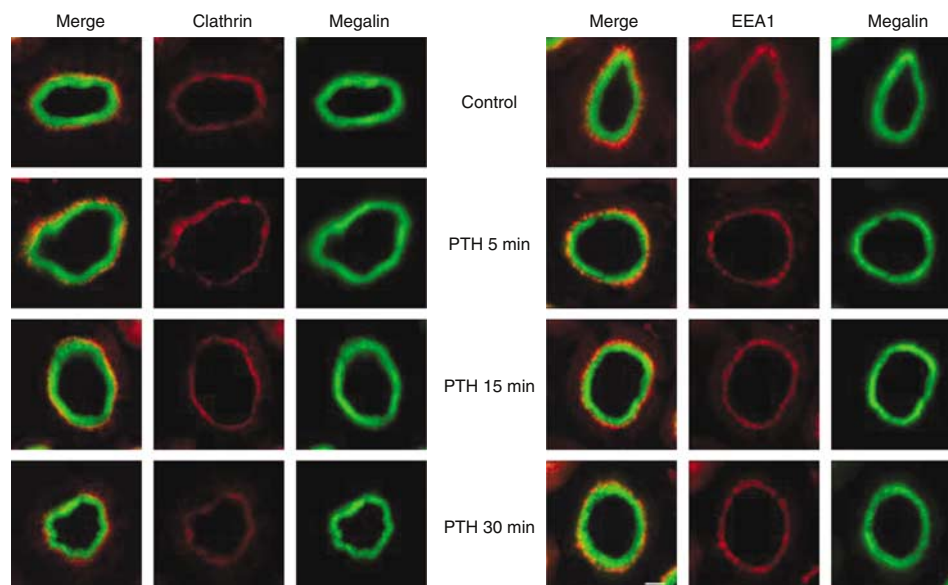


**Figure 5 | Localization of megalin (green label), clathrin (red label), and EEA1 (red label) in S1 segments of superficial nephrons from control rats and rats injected with PTH; cryostat sections, immunofluorescence.** Megalin is abundant and seen throughout the entire length of the BBM, clathrin is found below the brush border, and EEA1 slightly deeper in the cells. No difference was seen for megalin staining between control and treated animals. Bar =  $\sim 10 \mu\text{m}$ .



**Figure 6 | Localization of insulin in S1 proximal tubular cells; cryostat sections, immunofluorescence.** (a) Normally fed rats, (b) rats starved for 18 h, and (c) rats that were starved for 18 h and injected with insulin 5 min before perfusion fixation. Endogenous insulin was abundant in S1 proximal tubular cells in normally fed animals but not detected in starved animals. Insulin injected in starved rats was readily detected in subapical vesicles. Bar =  $\sim 50 \mu\text{m}$ .

## MATERIALS AND METHODS

### Animals

All animal studies were according to Swiss Animal Welfare laws and approved by the local Cantonal Veterinary Authority of Zurich. The experiments were performed with male Wistar rats (120–150 g). The rats were kept on a low-phosphate diet (0.1%  $\text{P}_i$  content) (Kliba AG, Switzerland) for 3 days to upregulate NaPi-IIa in the BBM of all proximal tubular segments as described previously.<sup>17</sup> In one group of animals used to stain for insulin, 18 h before PTH, HRP, or insulin injections, the food was removed in order to lower the animals' serum level of endogenous insulin.

A total of 53 rats were used divided into four separate experiments: experiment 1: injection of PTH after application of leupeptine; experiment 2: injection of PTH and insulin; experiment 3: injection of PTH and HRP; and experiment 4: injection of PTH and FITC-dextran.

Rats were anesthetized with thiopental (Pentothal, 100 mg/kg body weight) injected intraperitoneally, their

abdominal cavity was opened, and the aorta and vena cava were exposed. All animals received either saline as control or PTH (PTH 1-34 fragment,  $10 \mu\text{g}/100 \text{g}$  body weight (Sigma, St Louis, MO, USA)) injections as a bolus into the vena cava or the tail vein. The rats were perfused at each time point and fixed by perfusion.

Four separate experiments were performed and each experiment consisted of five groups with three animals per group.

**Experiment 1: injection of PTH and leupeptin.** Group 1 remained untreated and served as control animals. Groups 2 and 3 were injected with 1-34 PTH for 5/15 min before fixation as a single bolus injected into the vena cava. Groups 4 and 5 were injected into the tail vena as a single bolus with 1-34 PTH for 30/60 min before fixation. Additionally, group 5 received 6 mg leupeptin (Sigma) dissolved in 0.5 ml phosphate-buffered saline (PBS) as an injection into the tail vena before the PTH injection (into the tail vena as a single bolus).

**Experiment 2: injection of PTH and insulin.** Group 1 remained untreated and served as control animals. Group 2 was injected for 5 min with 1 U human insulin (Sigma) into the vena cava before fixation. Groups 3 and 4 were coinjected with 1-34 PTH and 1 U human insulin (Sigma) 5/15 min before fixation (as a single bolus injected into the vena cava). Group 5 was injected with 1-34 PTH into the tail vena. Fifteen minutes after PTH injection, 1 U human insulin (Sigma) was injected into the vena cava as a single bolus and animals fixed by perfusion after 15 min.

**Experiment 3: injection of PTH and HRP.** Group 1 remained untreated and served as control animals. Group 2 was injected with 0.75 ml of HRP-PBS solution (25 mg HRP,



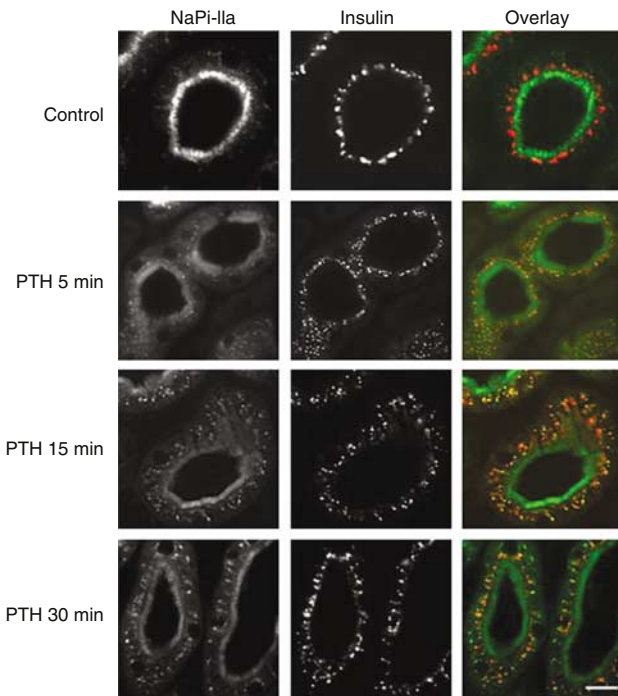


**Figure 7 | Double staining for NaPi-IIa (green label) and insulin (red label); cryostat sections, immunofluorescence.** After coinjection of PTH and insulin, distribution of NaPi-IIa during PTH treatment is similar to that of insulin. Intracellular NaPi-IIa and insulin overlap (orange/yellow) to a large extent. Bar = ~ 15  $\mu$ m.

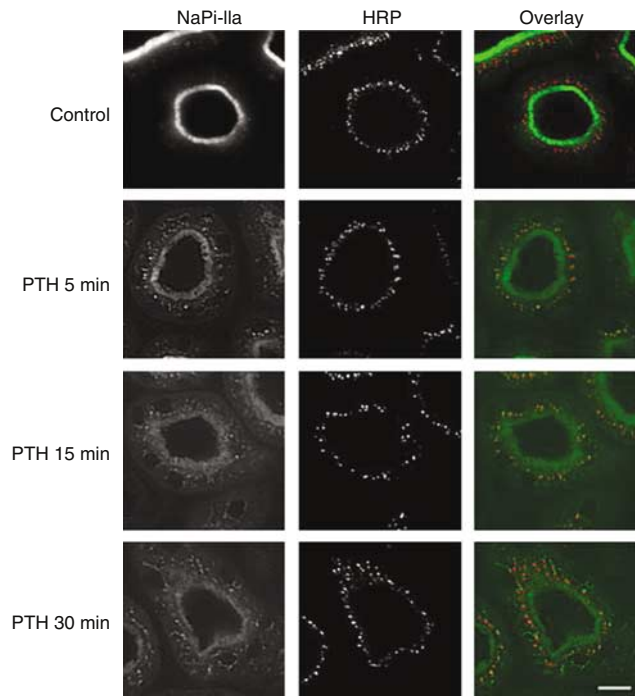


**Figure 8 | Double staining for NaPi-IIa (green label) and HRP (red label) in rats injected with PTH and HRP; cryostat sections, immunofluorescence.** NaPi-IIa-containing endocytic compartments do not overlap with HRP-labeled compartments. Bar = ~ 15  $\mu$ m.

Sigma type II, dissolved in 0.75 ml PBS; Sigma) into the vena cava 5 min before fixation. Groups 3 and 4 were coinjected with 1-34 PTH and HRP (as a single bolus injected into the vena cava) 5/15 min before fixation. Group 5 was injected with 1-34 PTH into the tail vena 30 min before fixation. Fifteen minutes after the PTH injection, HRP was injected into the vena cava as a single bolus.

**Experiment 4: injection of PTH and FITC-dextran.** Group 1 remained untreated and served as control animals. Group 2 was injected with 0.75 ml of FITC-dextran (10 kDa) solution (1.75 mg/100 g body weight, dissolved in 0.75 ml 0.9% NaCl; Molecular Probes, Eugene, OR) into the vena cava 5 min before fixation. Groups 3 and 4 were coinjected with 1-34 PTH and FITC-dextran (as a single bolus injected into the vena cava) 5/15 min before fixation. Group 5 was injected with 1-34 PTH into the tail vena 30 min before fixation. Fifteen minutes after the PTH injection, FITC-dextran was injected into the vena cava as a single bolus.

After treatment, all animals were fixed by vascular perfusion via the abdominal aorta, at a pressure of 0.4 bar, as described previously.<sup>29</sup> The fixative consisted of 3% paraformaldehyde, 0.1% glutaraldehyde, and 0.05% picric acid in 0.6M cacodylate buffer (pH 7.4; containing 3 mM MgCl<sub>2</sub> and adjusted to 300 mosmol/l with sucrose) and 4% hydroxyethyl starch in saline (HAES steril; Fresenius, Stans, Switzerland). After 5 min, the fixative was washed out by perfusion with hydrostatic pressure of 70 cm for 5 min with

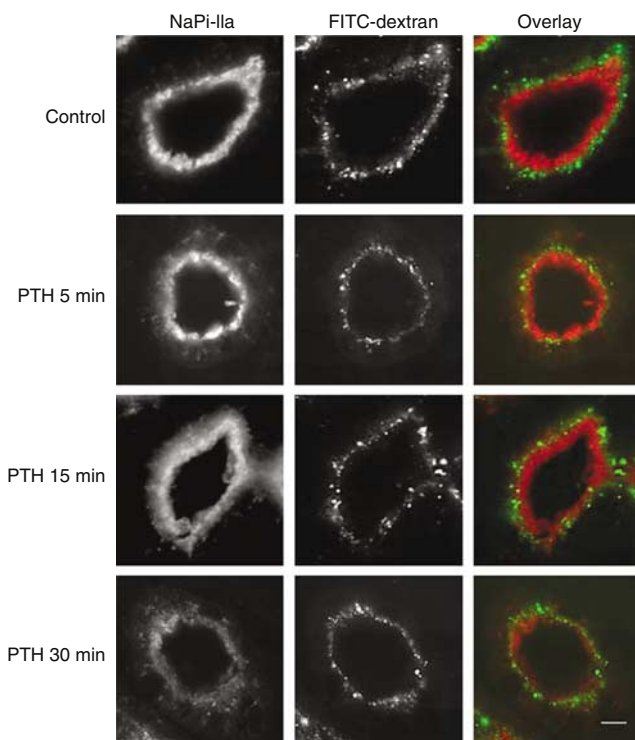


**Figure 9 | Double staining for NaPi-IIa (green label) and FITC-dextran (red label) in rats injected with PTH and FITC-dextran; cryostat sections, immunofluorescence.** NaPi-IIa-containing endocytic compartments do not overlap with FITC-dextran-labeled compartments. Bar = ~ 15  $\mu$ m.

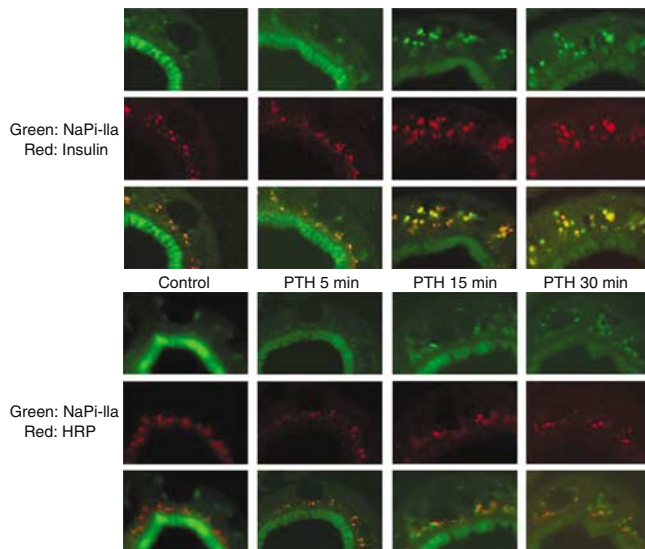


**Figure 10 | Double staining for NaPi-IIa and insulin (upper panel) and NaPi-IIa and HRP (lower panel) in control and PTH-treated rats; cryostat sections, immunofluorescence.** Distribution of endocytosed NaPi-IIa (green label) shows a high degree of overlap with insulin (red label) (overlap appears in orange-yellow) that is endocytosed via the receptor-mediated endocytotic pathway; compartments labeled with HRP (red label), representing the fluid-phase endocytotic pathway, do not overlap with endocytosed NaPi-IIa. Bar = ~ 15 μm.

Group	Treatment	Delay between PTH injection and fixation (min)	n
1	Untreated	—	3
2	1-34 PTH	5	3
3	1-34 PTH	15	3
4	1-34 PTH	30	3
5	Leupeptin 45 min+1-34 PTH	60	3

PTH: parathyroid hormone.

Group	Treatment	Delay between insulin injection and fixation (min)	n
1	Untreated	—	3
2	Insulin	5	3
3	1-34 PTH+insulin	5	3
4	1-34 PTH+insulin	15	3
5	1-34 PTH 30 min+insulin	15	3

PTH: parathyroid hormone.

cacodylate buffer. Kidneys were removed and subsequently used for analysis by immunohistochemistry.

**Immunohistochemistry**

Slices of fixed kidneys were frozen in liquid propane and cooled with liquid nitrogen. Sections, 3 μm thick, were cut at -22°C on a cryomicrotome, mounted on chromalum/gelatine-coated glass slides, thawed, and kept in cold PBS until use. Before immunofluorescence staining, sections were

Group	Treatment	Delay between HRP injection and fixation (min)	n
1	Untreated	—	3
2	HRP/PBS	5	3
3	1-34 PTH+HRP	5	3
4	1-34 PTH+HRP	15	3
5	1-34 PTH 30 min+HRP	15	3

HRP: horseradish peroxidase; PBS: phosphate-buffered saline; PTH: parathyroid hormone.

Group	Treatment	Delay between HRP injection and fixation (min)	n
1	Untreated	—	2
2	FITC-dextran/PBS	5	3
3	1-34 PTH+FITC-dextran	5	3
4	1-34 PTH+FITC-dextran	15	3
5	1-34 PTH 30 min+FITC-dextran	15	3

HRP: horseradish peroxidase; FITC: fluorescein isothiocyanate; PBS: phosphate-buffered saline; PTH: parathyroid hormone.

washed three times for 10 min with 50 mM NH<sub>4</sub>Cl in PBS and then pretreated with blocking solution (PBS with 0.1% bovine serum albumin containing 0.02% Triton X-100) for 10 min. After blocking, sections were washed three times in PBS and incubated overnight at 4°C with a rabbit anti-rat antiserum against the NaPi-IIa protein<sup>30</sup> diluted 1:1000, with a rabbit anti-megalin antiserum (kind gift of Dr Ziak and Dr Roth, Institute of Pathology, University of Zurich) diluted 1:10 000, with a rabbit anti-rat NHE3 antiserum (kindly provided by Dr Orson W Moe, University of Texas Southwestern Medical Center, Dallas, TX, USA) at a dilution of 1:1000, or with a mouse anti-rabbit NHE3 monoclonal antibody (clone 2B9; Chemicon International, Temecula, CA) diluted 1:50. All primary antibodies were diluted in blocking solution and incubated overnight at 4°C. For double staining, the following mouse monoclonal antibodies were diluted in a PBS/bovine serum albumin solution containing the NaPi-IIa antiserum: anti-HRP (Sigma) (1:250); anti-EEA1 (BD Transduction Lab, Pharmingen, Franklin Lakes, NJ, USA) and anti-clathrin (BD Transduction Lab) (both 1:100); and anti-Ig $\mu$  120 antibody (kindly provided by Dr I Melman, Yale University) and anti-insulin (Sigma) (both 1:50). Sections were then rinsed three times with PBS and covered for 45 min at 4°C with the secondary antibodies. Swine anti-rabbit IgG conjugated to FITC (Dakopatts, Glostrup, Denmark) was diluted 1:50 and goat anti-mouse IgG conjugated to Cy3 (Jackson ImmunoResearch Laboratories, West Grove, PA, USA) was diluted 1:500, both in PBS/3% milk powder. Double stainings of NaPi-IIa or NHE3 with  $\beta$ -actin filaments were achieved by adding rhodamine-phalloidin (Molecular Probes), at a dilution of 1:50 in the solution containing FITC-labeled secondary antibodies. Finally, the sections were rinsed three times with PBS, coverslipped using DAKO-Glycergel (Dakopatts) containing 2.5% 1,4-diazabicyclo[2.2.2]octane (Sigma) as a fading retardant, and studied either on an epifluorescence microscope (Polyvar, Reichert-



Jung, Austria) or on a confocal microscope (Leica SP1 UV CLSM).

#### ACKNOWLEDGMENTS

This study was supported by a grant from the Swiss National Research Foundation to HM (31-65397.01) and the 6th European Frame Work EuReGene Project (005085) to CAW and HM.

#### REFERENCES

- Murer H, Forster I, Biber J. The sodium phosphate cotransporter family SLC34. *Pflügers Arch* 2004; **447**: 763–767.
- Murer H, Hernando N, Forster I, Biber J. Proximal tubular phosphate reabsorption: molecular mechanisms. *Physiol Rev* 2000; **80**: 1373–1409.
- Murer H, Hernando N, Forster I, Biber J. Regulation of Na/Pi transporter in the proximal tubule. *Annu Rev Physiol* 2003; **65**: 531–542.
- Bacic D, Capuano P, Baum M et al. Activation of dopamine D1-like receptors induces acute internalization of the renal Na<sup>+</sup>/phosphate cotransporter NaPi-IIa in mouse kidney and OK cells. *Am J Physiol Renal Physiol* 2005; **288**: F740–F747.
- Murer H. Functional domains in the renal type IIa Na/Pi-cotransporter. *Kidney Int* 2002; **62**: 375–382.
- Traebert M, Roth J, Biber J et al. Internalization of proximal tubular type II Na-P<sub>i</sub> cotransporter by PTH: immunogold electron microscopy. *Am J Physiol Renal Physiol* 2000; **278**: F148–F154.
- Pfister MF, Ruf I, Stange G et al. Parathyroid hormone leads to the lysosomal degradation of the renal type II Na/Pi cotransporter. *Proc Natl Acad Sci USA* 1998; **95**: 1909–1914.
- Keusch I, Traebert M, Lötscher M et al. Parathyroid hormone and dietary phosphate provoke a lysosomal routing of the proximal tubular Na/Pi-cotransporter type II. *Kidney Int* 1998; **54**: 1224–1232.
- Pfister MF, Lederer E, Forgo J et al. Parathyroid hormone-dependent degradation of type II Na<sup>+</sup>/Pi cotransporters. *J Biol Chem* 1997; **272**: 20125–20130.
- Lötscher M, Scarpetta Y, Levi M et al. Rapid downregulation of rat renal Na/P<sub>i</sub> cotransporter in response to parathyroid hormone involves microtubule rearrangement. *J Clin Invest* 1999; **104**: 483–494.
- Christensen EI, Birn H. Megalin and cubilin: synergistic endocytic receptors in renal proximal tubule. *Am J Physiol Renal Physiol* 2001; **280**: F562–F573.
- Christensen EI, Birn H. Megalin and cubilin: multifunctional endocytic receptors. *Nat Rev Mol Cell Biol* 2002; **3**: 256–266.
- Piwon N, Gunther W, Schwake M et al. ClC-5 Cl<sup>-</sup>-channel disruption impairs endocytosis in a mouse model for Dent's disease. *Nature* 2000; **408**: 369–373.
- Bacic D, Capuano P, Gisler SM et al. Impaired PTH-induced endocytotic down-regulation of the renal type IIa Na<sup>+</sup>/P<sub>i</sub>-cotransporter in RAP deficient mice with reduced megalin expression. *Pflügers Arch* 2003; **446**: 475–484.
- Bachmann S, Schlichting U, Geist B et al. Kidney-specific inactivation of the megalin gene impairs trafficking of renal inorganic sodium phosphate cotransporter (NaPi-IIa). *J Am Soc Nephrol* 2004; **15**: 892–900.
- Orlando RA, Rader K, Authier F et al. Megalin is an endocytic receptor for insulin. *J Am Soc Nephrol* 1998; **9**: 1759–1766.
- Levi M, Lötscher M, Sorribas V et al. Cellular mechanisms of acute and chronic adaptation of rat renal P<sub>i</sub> transporter to alterations in dietary P<sub>i</sub>. *Am J Physiol* 1994; **267**: F900–F908.
- Biemesderfer D, DeGray B, Aronson PS. Active (9.6 s) and inactive (21 s) oligomers of NHE3 in microdomains of the renal brush border. *J Biol Chem* 2001; **276**: 10161–10167.
- Amemiya M, Loffing J, Lotscher M et al. Expression of NHE-3 in the apical membrane of rat renal proximal tubule and thick ascending limb. *Kidney Int* 1995; **48**: 1206–1215.
- Yang LE, Maunsbach AB, Leong PK et al. Differential traffic of proximal tubule Na<sup>+</sup> transporters during hypertension or PTH: NHE3 to base of microvilli vs. NaPi2 to endosomes. *Am J Physiol Renal Physiol* 2004; **287**: F896–F906.
- Willnow TE, Nykjaer A, Herz J. Lipoprotein receptors: new roles for ancient proteins. *Nat Cell Biol* 1999; **1**: E157–E162.
- Nykjaer A, Dragun D, Walther D et al. An endocytic pathway essential for renal uptake and activation of the steroid 25-(OH) vitamin D<sub>3</sub>. *Cell* 1999; **96**: 507–515.
- Nykjaer A, Fyfe JC, Kozyraki R et al. Cubilin dysfunction causes abnormal metabolism of the steroid hormone 25(OH) vitamin D<sub>3</sub>. *Proc Natl Acad Sci USA* 2001; **98**: 13895–13900.
- Norden AG, Lapsley M, Igarashi T et al. Urinary megalin deficiency implicates abnormal tubular endocytic function in Fanconi syndrome. *J Am Soc Nephrol* 2002; **13**: 125–133.
- Biemesderfer D, Nagy T, DeGray B, Aronson PS. Specific association of megalin and the Na<sup>+</sup>/H<sup>+</sup> exchanger isoform NHE3 in the proximal tubule. *J Biol Chem* 1999; **274**: 17518–17524.
- Kempson SA, Helmlé C, Abraham MI et al. Parathyroid hormone action on phosphate transport is inhibited by high osmolality. *Am J Physiol* 1990; **258**: F1336–F1344.
- Brown D, Weyer P, Orci L. Vasopressin stimulates endocytosis in kidney collecting duct principal cells. *Eur J Cell Biol* 1988; **46**: 336–341.
- Katsura T, Verbavatz JM, Farinas J et al. Constitutive and regulated membrane expression of aquaporin 1 and aquaporin 2 water channels in stably transfected LLC-PK1 epithelial cells. *Proc Natl Acad Sci USA* 1995; **92**: 7212–7216.
- Dawson TP, Gandhi R, Le Hir M, Kaissling B. Ecto-5'-nucleotidase: localization in rat kidney by light microscopic histochemical and immunohistochemical methods. *J Histochem Cytochem* 1989; **37**: 39–47.
- Custer M, Lötscher M, Biber J et al. Expression of Na-P<sub>i</sub> cotransport in rat kidney: localization by RT-PCR and immunohistochemistry. *Am J Physiol* 1994; **266**: F767–F774.